Tribological and corrosion wear of graphite ring against Ti6Al4V disk in artificial sea water

I. Serre, N. Celati, R. M. Pradeilles-Duval

Tribological and corrosion wear of graphite ring against Ti_6Al_4V disk in artificial sea water

I. Serre [a,b], N. Celati [a], R.M. Pradeilles-Duval [b,*]

[a] *DGA/DCE/centre technique d'Arcueil, 16 bis av. Prieur de la Côte d'Or, 94114 Arcueil Cedex, France*
[b] *Laboratoire de Mécanique des Solides, CNRS UMR 7649, Ecole Polytechnique, 91128 Palaiseau, France*

Abstract

Severe degradations result from the friction of two antagonists in sea water environment. It is proposed to evaluate materials resistance to wear with a tribocorrosion experimental set-up which is mechanically and electrochemically instrumented. The method is illustrated with graphite and Ti_6Al_4V.

The deposition of graphite on Ti_6Al_4V samples is observed and modifies the contact characteristics. Processes of graphite wear due to mechanical effect are characterised. Observations clearly indicate that Ti_6Al_4V degradations depend on the electrochemical potential imposed and more precisely on the electrochemical conditions in the contact zone.

Keywords: Planar contact; Tribocorrosion; Graphite; Ti_6Al_4V

1. Introduction

In marine environment, planar contacts which should have sealing capacity are found in ring-on-disk systems, pumps, packers of boat, etc. Therefore, the evaluation of the life durability of the structures requires to identify the degradation mechanisms and to formulate wear laws for antagonists in contact in a corrosive environment [1,2]. Tribocorrosion experiments should allow for the identification and the estimation of the material parameters required for the wear laws.

In the class of problems considered, two rings are in contact and rotate, one with respect to the other. In the contact region, friction induces material wear, tampering with waterproofing and the sealing capacity of the system. Classical pin-on-disk tribocorrosion experiments are not relevant to this class of problems because of the difference in the contact geometry, in the time evolution, in the spatial distribution of the pressure, in the wear debris displacement, which are all paramount wear parameters. For these reasons, a ring-on-disk tribocorrosion experimental set-up was developed with an electrochemical and a mechanical instrumentation [2,3]. These experiments enable us to study degradation processes of materials submitted to friction in sea water.

Classically, the tribocorrosion experiments are carried out with one antagonist made of alumina [1,4–6] despite the well-known influence of the physical, chemical and mechanical reactions on wear and friction between the specific materials [7,8]. Alumina is chosen because it is electrochemically inert simplifying the interpretation of the electrochemical measurements. Because of its strong mechanical properties in comparison with those of the second antagonist material, no material loss and no significant degradation are observed for alumina. The tribocorrosion experiments considered here were specifically designed for the two materials used in the real structure namely, graphite and a titanium alloy, Ti_6Al_4V.

The purpose of this paper is to study and to understand the wear behaviour in a corrosive environment, i.e. the tribocorrosion for a ring on disk contact. In this paper, we have focused on the evolution of the friction coefficient and the wear of the two antagonists.

2. Materials and experimental conditions

2.1. Description of materials

The two antagonists considered are a sintered graphite and a titanium alloy, Ti_6Al_4V. The elastic properties of the two materials as obtained from a resonance frequency method [9] are given elsewhere.

* Corresponding author.
E-mail addresses: serre@lms.polytechnique.fr (I. Serre), rachel@lms.polytechnique.fr (R.M. Pradeilles-Duval).

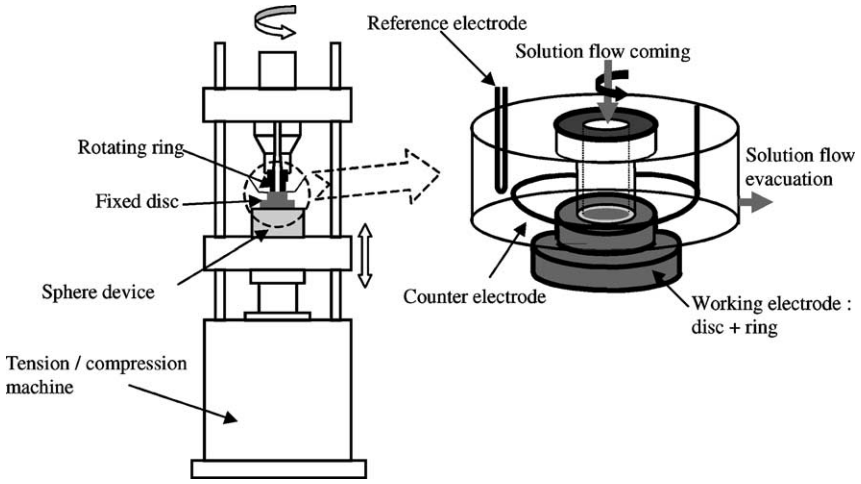

Fig. 1. Ring-on-disk tribometer principle.

The ring is cut from a cube of Hot Isostatically Pressed (HIP) graphite. The material is elastic brittle and isotropic [10]. Elasticity limits of 38 and 160 MPa are measured in traction and in compression, respectively. Young's modulus of the graphite is 13 GPa and Poisson's ratio is 0.13 [2].

The disk is made of Ti_6Al_4V, having Poisson's ratio of 0.3 and Young's modulus of 120 GPa. This material has not sustained any treatment so that its microstructure is standard α/β duplex mixture. Its elasticity limit is around 900 MPa.

2.2. Experimental device description

Experiments are carried out with ring on disk tribocorrosimeter developed by "le centre technique d'Arcueil" [2,3]. This tribocorrosimeter (Fig. 1) consists in a fixed disk and a rotating ring. The contact between the two antagonists is maintained by applying a normal pressure. An electrochemical cell permits corrosion experiments in artificial sea water with prescribed electrochemical conditions.

The annulus has an average radius of 8 mm. The width of the contact zone is 3 mm. The fixed disk is assembled with a sphere which has the function of a kneecap. As a result, during the annulus rotation, it is possible to obtain a planar contact by correction of the parallelism defects between the disk and the annulus. These defects are inherent to the set-up of the antagonists or are generated by the wear phenomena. A series of short experiments has permitted to establish that the friction zones and wear are independent of the angular position on the contact surface and that the contact is really planar after few seconds.

During the experiments, the friction coefficient and the cumulated wear (the sum of ring wear and disk wear) of the two antagonists are measured. After the experiments, the total wear of the disk is evaluated by profilometry. The height of the annulus is measured before and after each experiment to obtain the total wear of the graphite annulus.

All the experiments were performed at room temperature in a circulating artificial sea water, i.e. A3 solution (NaCl solution to 30 g/l buffered at pH 8 according to standard NFA 91 411). A three-electrode set-up (Fig. 1) enables to impose different potentials on the exposed surface of both samples and to measure the current [2]. All electrochemical potential values are given in what follows with reference to the Ag/AgCl saturated KCl electrode.

The bath is stirred continuously during the experiment, with the help of a pump, to ensure the stability of the artificial sea water characteristics. As a result, there is homogeneity and stability of the pH but also of the displacements of the wear debris out of the contact area.

The average pressure applied between the two antagonists is constant during the experiments and is equal to 5.3 MPa. This load value is representative of the applied pressure in the industrial case and ensures that the two materials are in their elastic range of deformation.

The graphite annulus rotates at 40 rpm, which corresponds to a mean velocity of 0.033 m/s. In addition, most of experiments last for 6 h unless otherwise stated.

3. Experimental results and discussion

3.1. Friction coefficient

At the end of the experiments, the friction coefficient ranges between 0.12 and 0.22 whatever the electrochemical conditions. It increases during transient phase of approximately 20 min. The initial values of the friction coefficient given in Table 1 are obtained after this transient stage. The evolution in time of the friction coefficient beyond the first transient is towards a stable value which does not depend strongly on the electrochemical potential value (-1.010, -0.060 and 0.140 V). For the other studied prescribed potential (-0.810, -0.210 V and free potentials

Table 1
Friction coefficient function to the electrochemical conditions of experiment

Electrochemical conditions	Initial value of the experiment	End value of the experiment
Imposed potential of −1.010 V	0.15 ± 0.02	0.15 ± 0.01
Imposed potential of −0.810 V	0.18 ± 0.02	0.16 ± 0.09
Imposed potential of −0.210 V	0.13 ± 0.04	0.12 ± 0.01
Open circuit	0.17 ± 0.02	0.16 ± 0.04
Imposed potential of −0.060 V	0.13 ± 0.03	0.16 ± 0.04
Imposed potential of 0.140 V	0.14 ± 0.04	0.22 ± 0.04

(around −0.100 V)), the friction coefficient does not reach a stable value during the experiment and keeps on increasing.

3.2. Wear

The two materials experience with damage and material loss during the tribocorrosion experiments. The following subsections focus on the specific wear of the two antagonists.

3.3. Graphite wear

We observe (Table 2) that the material loss of the graphite ring tends to decrease as the prescribed electrochemical potential is increased except for the experiments at an applied potential of −0.810 V. We note that, the smaller the friction coefficient, the larger the material loss of graphite.

Electrochemical reactions of the artificial sea water occur on the graphite surface. But, dissolution or oxidation of graphite cannot happen under atmospheric pressure and at room temperature [11]. Thus, the origin of graphite material loss is mechanical. Physical and chemical surface of the Ti_6Al_4V disk is different depending on the prescribed electrochemical potential. So this evolution of the properties of the antagonist can explain the small evolution of the graphite wear with the prescribed electrochemical potential.

After experiment, we observe small microscopic graphite particles (<10 μm) and macroscopic graphite lengthened chips (about 1 mm) (Figs. 2 and 3). After 5 or 20 min experiments, we observe by scanning electron microscopy (SEM) only microscopic graphite debris on the edges of the Ti_6Al_4V friction zone. After 6 h experiments, microscopic debris are

Table 2
Material loss of the graphite ring after 6 h experiments function electrochemical conditions of experiment

Electrochemical conditions	Loss height of graphite ring (μm)	Matter loss of graphite ring (mm^3)
Imposed potential of −1.010 V	23 ± 3	3.4 ± 0.5
Imposed potential of −0.810 V	11 ± 4	1.6 ± 0.6
Imposed potential of −0.210 V	23 ± 10	3.5 ± 1.5
Open circuit	19 ± 10	2.9 ± 1.5
Imposed potential of −0.060 V	20 ± 2	3.0 ± 0.4
Imposed potential of 0.140 V	17 ± 4	2.5 ± 0.6

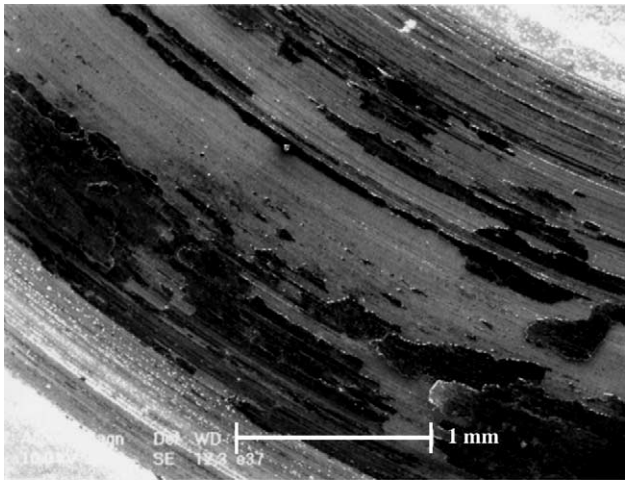

Fig. 2. Wear track of Ti_6Al_4V disk: presence of graphite debris.

observed in the artificial sea water solution as well as in the Ti_6Al_4V friction zone. Macroscopic chips are observed after 6 h experiment on the friction zone of the Ti_6Al_4V disk (Figs. 2 and 3). On this macroscopic debris, cracks in the slip-parallel and slip-perpendicular directions are present (Fig. 4).

From these after-experiment analysis, we deduce that the graphite matter removal occurs in two ways: small microscopic particles and macroscopic lengthened chips. These types of matter removal seem to occur simultaneously during experiments. But only microscopic debris appear at the very beginning of the experiments.

In the graphite friction zone, one observes microscopic cracks perpendicular to the friction movement (Fig. 5). In addition, the presence of cracks which propagate in the direction of movement suggests the possibility that the removal of graphite is carried out by macroscopic chipping according to the direction of friction. Moreover, because of the presence of cracks on the macroscopic chips and

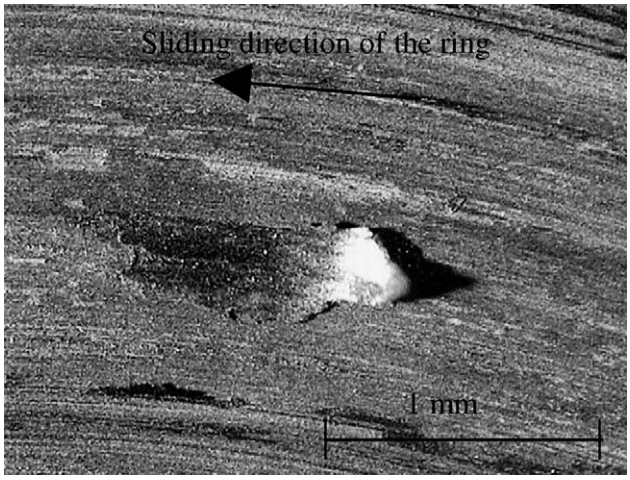

Fig. 3. Macroscopic graphite debris on a Ti_6Al_4V disk.

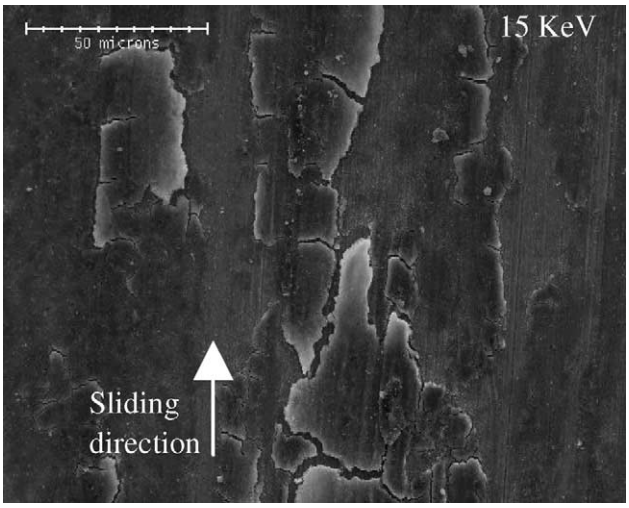

Fig. 4. Cracks perpendicular to the sliding direction on graphite debris.

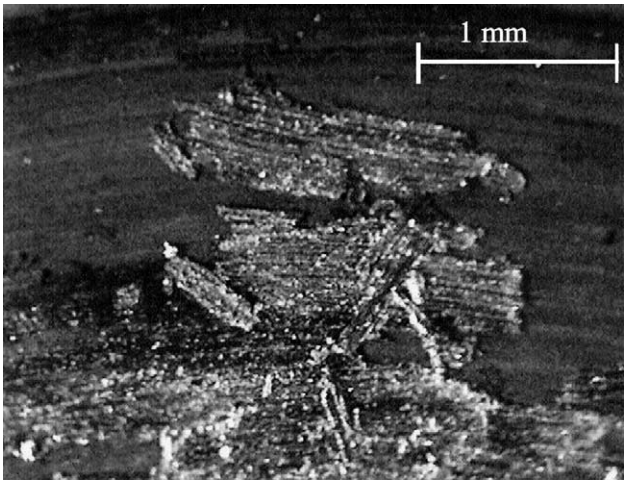

Fig. 6. Friction scratches on graphite debris.

because we do not collect any macroscopic debris by filtering the artificial sea water after experiment, the macroscopic debris are destroyed in the contact. After this process, we think that they are ejected out of the contact zone. So, microscopic debris are produced during long experiments, either directly or from cracking of the macroscopic debris.

Furthermore, the macroscopic debris, observed in the contact zone, present marked scratches of friction (Fig. 6). This observation shows paradoxically that debris are in the contact area for such a long time that they participate to friction without being cracked. The adherence between the debris of graphite and the alloy of Ti_6Al_4V induces local friction of graphite against graphite, which explains the small friction coefficient.

It must be underline that the wear of the graphite is not homogeneous in the width of the contact zone. Indeed, along the internal edge of the graphite ring, irregular damages are present while they are not observed along external edge (Fig. 7). This might be due at least in part to the wear debris evacuation which is not of the same kind inside and outside the friction track due to the circulation of artificial sea water (from outside to inside the ring). Other explanations can be the dimension of the zone of the debris evacuation, i.e. the length of the evacuation front or the difference in linear velocity between the internal edge and the external edge of the contact zone (0.027–0.039 m/s) causing different wear rates. Lastly, non-homogeneity in pressure across contact zone might influence the spatial evolution of the wear rate too [2,12].

Furthermore, a profilometry of the graphite friction zone is carried out perpendicularly to the friction direction. The roughness changes during the experiments: the Ra of the graphite increases from 0.2 μm before experiment to 0.4–0.6 μm after experiment while the Ra of the disk reaches approximately 0.3–0.6 μm, after experiment. This increase is probably due to the heterogeneity of the wear of the graphite surface and to the roughness of the Ti_6Al_4V disk.

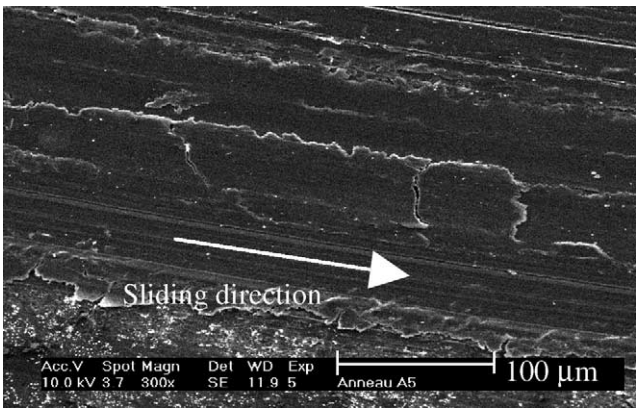

Fig. 5. Friction track of the graphite ring: cracking of the graphite.

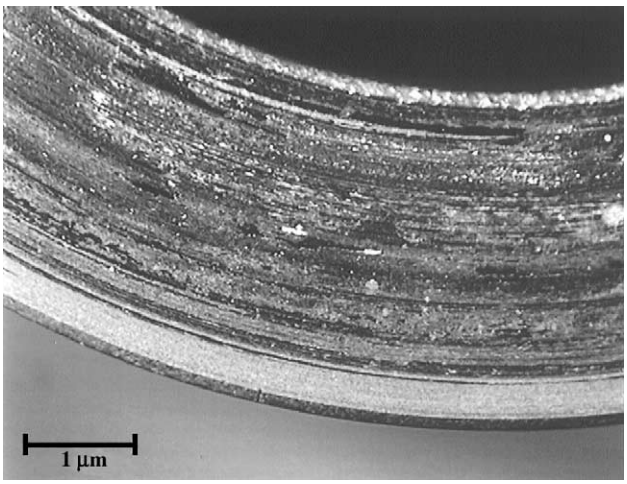

Fig. 7. Friction zone of the graphite ring: different wear on internal and external edges of ring.

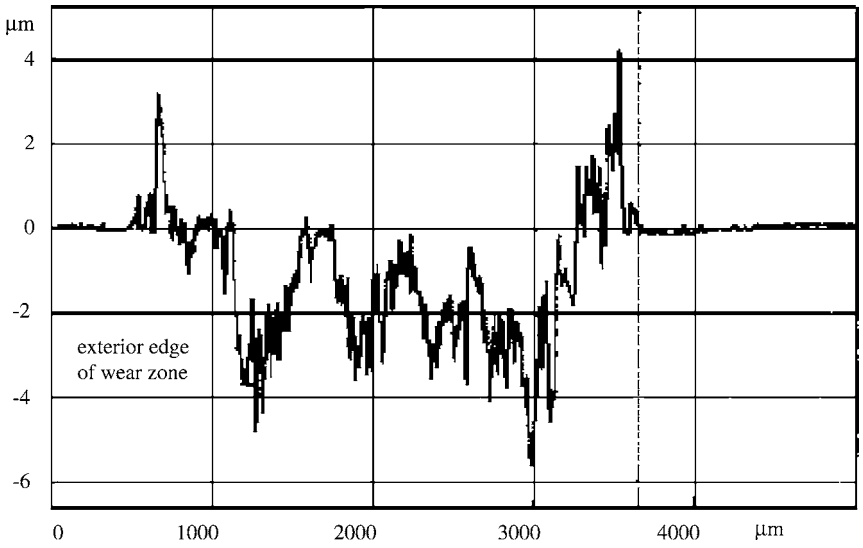

Fig. 8. Profilometry of the wear track for the Ti_6Al_4V sample: experiment at electrochemical potential of 0.140 V.

3.3.1. Ti_6Al_4V wear

The material loss of the Ti_6Al_4V disk is measured by profilometry. Four radial measurements are carried out every 90° around the disk. We assume that the eroded volume corresponds to the product of the average surface under the initially measured level of the sample multiplied by the mean length of the friction track. Analyses of Ti_6Al_4V disks indicate that the material loss of Ti_6Al_4V is strongly dependent on electrochemical conditions. With electrochemical potential of 0.140 V, experimental results give a material loss of $0.22 \pm 0.06\,mm^3$. It must be note that this material loss is not homogeneous across the track and is located in a preferential way nearby the edges of the friction zone (Fig. 8) as yet highlighted by Walter and Plitz [13]. At a potential lower than −0.060 V, the Ti_6Al_4V wear corresponds to grooves whose depth is between 3 and 5 µm. They are located along the edges of the friction zone (Fig. 9). For lower potentials (free corrosion potential around −0.100 V with our electrochemical measurement configuration, potential of −0.210, −0.810, −1.010 V), the grooves mainly have lower depth (<2 µm). We note, the presence of bulb edges, along the friction track, after the experiments at 0.140 V.

Furthermore, observations by SEM of the contact track (Fig. 2) clearly indicate a low thickness graphite deposit.

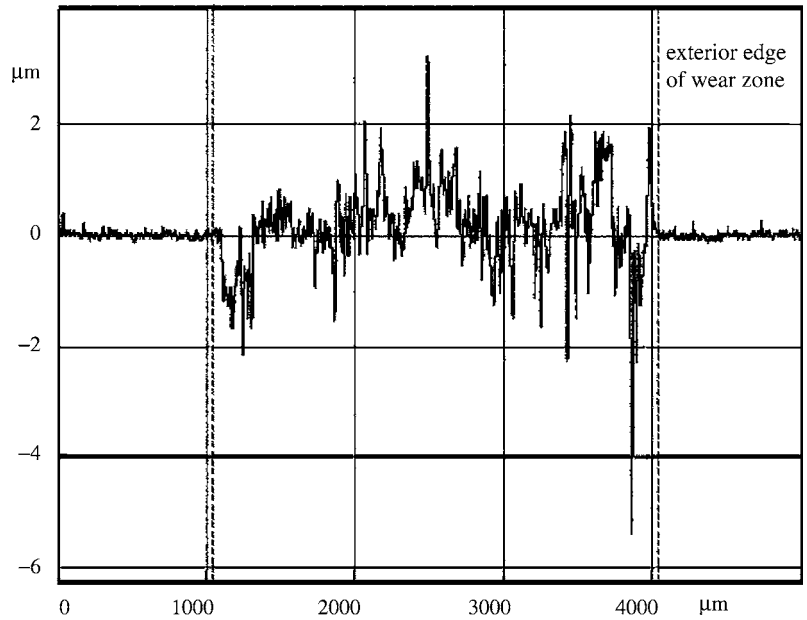

Fig. 9. Profilometry of the wear track for the Ti_6Al_4V sample: experiment at electrochemical potential of −0.060 V.

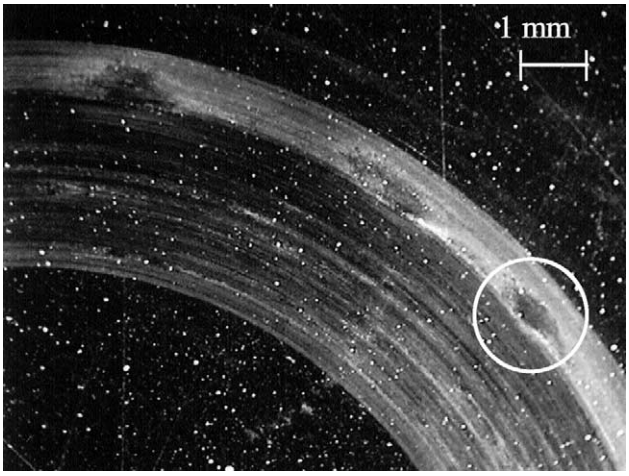

Fig. 10. Graphite clusters on the wear track of the Ti_6Al_4V sample.

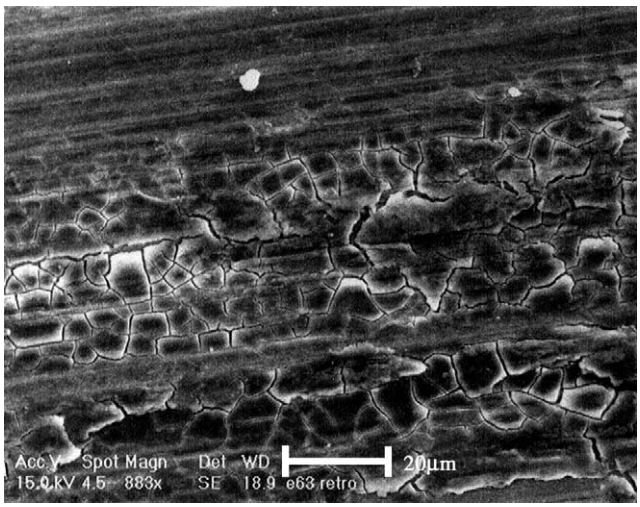

Fig. 11. Products of corrosion on Ti_6Al_4V friction zone.

This deposit is adherent. Then, it corresponds to graphite transferred on the disk surface rather than graphite debris. However, the study of the trail after some experiments (Fig. 10) exhibits very thin graphite clusters. They have oval form with the major axis along the direction of the slip. Since several cleanings with ultrasounds can not remove them, we deduce that they are strongly adherent with Ti_6Al_4V, at least more adherent than a part of the transferred graphite which goes away with cleanings. The Ti_6Al_4V roughness increases from a Ra included between 0.02 and 0.04 µm before experiment, to a Ra between 0.3 and 0.6 µm after experiment. Probably, this increase is associated for a part to the presence of the graphite deposit. In optical microscopy we observe that the Ti_6Al_4V disk presents friction scratches in the slip direction which are not uniform across the contact area. Some zones do not present observed scratches by SEM. This confirms that the friction is not uniform because of the non-uniform contact pressure and also because of the graphite deposit and macroscopic graphite debris presence. Nevertheless, observations by optical and SEM of the disks show that the friction scratches, the grooves and the material loss are homogeneous according to the rotation angle.

For the experiments at free potential or at an imposed potential of 0.140 and −0.060 V, the corrosion products are observed in the friction zone and particularly on the edges of the friction track (Figs. 11 and 12). These corrosion products are not due to an ageing of the samples after experiment because none is observed except on the friction track. Chipping and friction scratches are also observed (Fig. 12). In general, the damaging phenomena occur on corrosion products, located on the external edge of the wear track. A chemical analysis of these corrosion products was performed by SEM analysis. Phosphorus, oxygen, sodium and chlorine were detected. Titanium, aluminium and vanadium are also detected in some cases. According to the thickness of the corrosion products and with regards with the accuracy of the chemical analyses by SEM method, the presence of these three latter elements may be due either to the presence of Ti_6Al_4V which constitutes the disk or to their real presence in the corrosion products. To conclude of their presence or not in the corrosion products, new chemical analyses with different techniques should be experimented even if the roughness and the non-flatness of the wear contact of the Ti_6Al_4V disk prove to be awkward. Chemical analyses suggest also that some corrosion products contain carbon. It comes from graphite, in particular from the transferred graphite or the graphite debris on the Ti_6Al_4V disk or from the friction between the corrosion products against the graphite ring.

On the friction track, an increase of the concentration of oxygen is always observed by SEM. We find much more oxygen near the edges of this zone. Moreover, in this area, we observe an increase of the concentration of phosphorus and to a less extent, chlorine and sodium. These latter three elements are not related to the presence or not of products of corrosion.

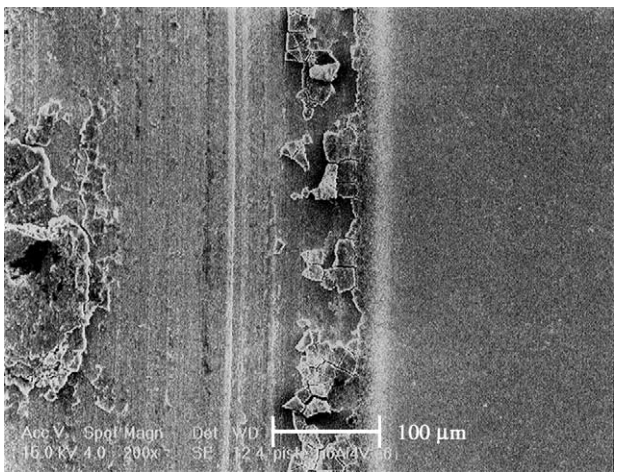

Fig. 12. Products of corrosion on the external edge of the Ti_6Al_4V friction zone.

This latter observation and the presence of the corrosion products actually show the existence of electrochemical reactions for titanium alloy, namely nearby the edges of the friction zone in term of reactions between the Ti_6Al_4V surface and the solution A3. Different electrochemical reactions (anodic or cathodic) reactions take place, according to the electrochemical conditions.

The wear of the Ti_6Al_4V disk especially depends on the electrochemical potential. At a potential of 0.140 V, the Ti_6Al_4V disk presents a material loss which is measured by profilometry (Fig. 8). This material loss cannot be obtained through a mechanical phenomenon only, because of the higher mechanical properties of Ti_6Al_4V compared to those of graphite and because of the small applied contact pressure (5 MPa on average) in comparison with the limit of elasticity of the Ti_6Al_4V (around 900 MPa). Other experiment results with Ti_6Al_4V against smooth material were performed with Ti_6Al_4V rubbing against ultra high molecular weight polyethylene (UHMWPE) [16–18]. The wear i.e. the material loss of Ti_6Al_4V was observed while polyethylene has low mechanical characteristics (Young's modulus approximately 27–67 MPa) and the loading applied is below 20 MPa. Different experiments configurations in serum or in salt solution were carried out: pin on disk [16], cylinder on cylinder [17], or ring on disk [18]. Those papers underlined that titanium alloy wear was due to the low resistance of oxide films. Those experimental works highlighted that oxide removal, of strong hardness, acted like abrasive and contributed to the wear of the antagonists.

In our case, first, the electrochemical potential could induce a modification of Ti_6Al_4V surface properties by existence of different oxides films. Because mechanical characteristics of oxides film evolve with the electrochemical potential, consequently, a modification of the potential can induce a variation of the wear of the Ti_6Al_4V surface even if the two antagonists have very different mechanical characteristics. Second, in the ring-on-disk experiment, the contact is a priori macroscopically continuous between the two antagonists. So the depassivation/repassivation processes which are observed during a pin-on-disk experiment, could a priori not occur. Yet, by using a specific electrochemical montage, based on current/tension converters [2,19], we observe that, under friction, the contact between the two antagonists is not electrochemically perfect [2]. This means local processes of depassivation/repassivation of the Ti_6Al_4V by contact with the graphite. Thanks specifics experiments using current/tension converters and thanks electrochemical study of the two materials [2], we establish that during tribocorrosion experiments at 0.140 V, the measured current mainly corresponds to contribution of the anodic reactions (formation of titanium oxides) to the Ti_6Al_4V surface. Moreover, we check that for the experiments at 0.140 V, measurements of the Ti_6Al_4V material loss ($0.22 \pm 0.06\,mm^3$) are consistent with the material loss calculated with the measured current and Faraday's law ($0.20 \pm 0.05\,mm^3$) [2,20]. Consequently, in our case, the Ti_6Al_4V material loss is mainly due, at anodic potential to locally depassivation/repassivation phenomena in spite of a permanent macroscopic contact.

The corrosion products, like the graphite clusters, probably influence the friction and the wear by their properties particularly mechanical properties. This influence is all the more important since the pressure average of contact is small [7]. Indeed, surface properties influence the response of materials to friction and thus their wear [14–16]. Furthermore, the graphite transferred and the graphite clusters are adherent to the Ti_6Al_4V disk. So, they induce local friction of graphite against graphite ring which could explain the small friction coefficient.

4. Conclusion

A new tribocorrosion experimental set-up has been used to study materials wear for a ring in friction with a disk in sea water environment [2,3]. Observations at the end of the experiment permit to determine the process of material loss and degradation for the graphite ring and Ti_6Al_4V disk. We observe both graphite removal and graphite transferred on Ti_6Al_4V. Graphite removal consists in the creation of large chips which are either deposed on the Ti_6Al_4V surface or broken inside the contact area before being ejected in solution. The material loss of the Ti_6Al_4V disk depends on the electrochemical conditions: no significant material loss exists during experiments at cathodic potential. For the experiments at anodic potential, the electrochemical material loss is calculated using the measured current and the Faraday's law. This shows that the wear of Ti_6Al_4V is mainly due to the existence of depassivation/repassivation phenomena for a continuous macroscopic contact, i.e. in a ring on disk contact.

Acknowledgements

The authors wish to thank Mr Louchart of Centre Technique d'Arcueil (France) for his technical assistance. We are indebted to Mr. Keddam and Mr. Takenouti from the laboratory "Physique des Liquides et Electrochimie" for their help about the electrochemical set-up with the current/tension converters.

References

[1] G. Lederer, Modélisation tribomécanique du frottement en milieu agressif, Doctorate Thesis, Ecole Polytechnique, 1998.
[2] I. Serre, Contribution à l'étude des phénomènes d'usure par frottement en milieu marin, Doctorate Thesis, Ecole Polytechnique, 2000.
[3] I. Serre, R.M. Pradeilles Duval, N. Celati, Modélisation d'un contact graphite contre Ti_6Al_4V renforcé TiC en milieu marin artificiel: essais de tribocorrosion plan/plan de type anneau/disque, Bulletin du Cercle d'Etudes des Métaux, Matériaux Usure et Corrosion, tome 16 (19) (1999) 15.1–15.8.

[4] S. Mischler, P. Ponthiaux, A round robin on combined electrochemical and friction tests on alumina/stainless steel contacts in sulphuric acid, Wear 248 (2001) 211–225.
[5] P. Jemmely, S. Mischler, D. Landolt, Tribocorrosion behaviour of the Fe-17Cr stainless steel in acid and alkaline solutions, Tribol. Int. 32 (1999) 295–303.
[6] M.F. Lizandier, E. Lanza, A. Sebaoum, A. Giraud, P. Guiraldenq, Characterization of porosity of ceramic coatings assigned to applications in sea water with the evolution of their electrochemical behaviour under friction, Wear 153 (1992) 387–397.
[7] J.M. Georges, Frottement, usure et lubrification, CNRS Editions Eyrolles, 2000
[8] K. Kato, Wear in relation to friction: a review, Wear 241 (2000) 151–157.
[9] Standard test method for dynamic Young's modulus and Poisson ratio for advanced ceramics by impulse excitation of vibration, norme ASTM C 1259–94.
[10] Soc. Le Carbonne Loraine, France, Carbons and graphites for mechanical applications, technical notice for the use of graphite, 1998.
[11] J. Van Muyder, M. Pourbaix, Electrochemical Equilibrate at 25 °C Atlas, 1963.
[12] I. Serre, M. Bonnet, R.M. Pradeilles Duval, Modelling an abrasive wear experiment by the boundary element method, Compte-Rendu à l'Académie des Sciences, série IIb 329 (2001) 803–808.
[13] A. Walter, W. Plitz, The ring on disk method: clinical significance of a wear-screening test of biomaterials for hip joint alloplasty, in: S.M. Perren, E. Schneider (Eds.), Biomechanics: Current Interdiskiplinary Research, Nijhoff, Dordrecht, 1985, pp. 129–134.
[14] E. de Wit, D. Drees, P.Q. Wu, J.P. Celis, Lubricating reaction products on TiN coatings during sliding wear in phosphoric acid, Surf. Coatings Technol. 135 (2000) 8–13.
[15] H. Schmidt, A. Schminke, M. Schmiedgen, B. Baretzky, Acta Mater. 49 (2001) 487–495.
[16] A. Magnée, M. Douet, B. Forest, J. Rieu, Y. Corre, Influence de traitements de surface sur le comportement tribomécanique d'un alliage de titane pour prothèses osseuses, Bulletin du Cercle d'Etudes des Métaux, Matériaux Usure et Corrosion, tome 16 (19) (1999) 19.1–19.10.
[17] R.A. Buchanan, E.D. Rigney, J.M. Williams, Ion implantation of surgical Ti_6Al_4V for improved resistance to wear-accelerated corrosion, J. Biomed. Mater. Res. 21 (1987) 355–366.
[18] R. Martinella, S. Giovarnadi, G. Palombarini, M. Corchia, P. Delogu, R. Giorgi, C. Tosello, Wear behaviour of the couple polyethylene-Ti_6Al_4V: effects of the metallic surface preparation and nitrogen implantation, Nuclear Instrum. Meth. Phys. Res. B19/20 (1987) 23240.
[19] C. Deslouis, C. Gabrielli, B. Tribollet, Multi-channel potentiostatic control in electrochemistry: localised mass-transfer rates at the rotating disk electrode, Phys. Chem. Hydrodynamics 2 (1981) 23–30.
[20] D. Landolt, Corrosion et chimie des surfaces et des métaux, Presses Polytechniques et Universitaires Romandes, Alden Press, Oxford, 1997.